

A METHOD FOR DESIGNING MULTI-LAYER SHEET-BASED LIGHTWEIGHT FUNICULAR STRUCTURES

Yao LU¹, Thamer ALSALEM² and Masoud AKBARZADEH³

¹ Ph.D. Student, Polyhedral Structures Laboratory, School of Design, University of Pennsylvania, USA
yaolu61@upenn.edu

² Master's Student, School of Design, University of Pennsylvania, USA
tsa7@design.upenn.edu

³ Assistant Professor, Polyhedral Structures Laboratory, School of Design, University of Pennsylvania, USA
masouda@upenn.edu

Editor's Note: The first author of this paper is one of the four winners of the 2022 Hangai Prize, awarded for outstanding papers that are submitted for presentation and publication at the annual IASS Symposium by younger members of the Association (under 30 years old). It is published here with permission of the editors of the proceedings of the IASS Symposium 2022 "Innovation, Sustainability and Legacy", that was held in September 2022 in Beijing, China.

DOI: <https://doi.org/10.20898/j.iass.2022.018>

ABSTRACT

Multi-layer spatial structures usually take considerable external loads with a small material usage at all scales. Polyhedral graphic statics (PGS) provides a method to design multi-layer funicular polyhedral structures, and the structural forms are usually materialized as space frames. Our previous research shows that the intrinsic planarity of the polyhedral geometries can be harnessed for efficient fabrication and construction processes using flat-sheet materials. Sheet-based structures are advantageous over conventional space frame systems because sheets can provide more load paths and constrain the kinematic degrees of freedom of the nodes. Therefore, they are more capable of taking a wider variety of load cases compared to space frames. Moreover, sheet materials can be fabricated into complex shapes using CNC milling, laser cutting, water jet cutting, and CNC bending techniques. However, not all sheets are necessary as long as the load paths are preserved and the system does not have kinematic degrees of freedom. To find an efficient set of faces that satisfies the requirements, this paper first incorporates and adapts the matrix analysis method to calculate the kinematic degrees of freedom for sheet-based structures. Then, an iterative algorithm is devised to help find a reduced set of faces with zero kinematic degrees of freedom. To attest to the advantages of this method over bar-node construction, a comparative study is carried out using finite element analysis. The results show that, with the same material usage, the sheet-based system has improved performance than the framework system under a range of loading scenarios.

Keywords: polyhedral graphic statics, matrix analysis, sheet-based structure, form-finding, funicular structure, structural optimization

1. INTRODUCTION

Space frames, featured as lightweight and efficient, have been commonly practiced for creating long-span or cantilever structures. The recent development of three-dimensional graphic statics using polyhedral reciprocal diagrams, usually referred to as polyhedral graphic statics (PGS), provides an approach to designing complex and multi-layer 3D funicular frameworks while being aware of the internal force distribution [1]. The dimensions of the members can be determined based on their internal forces, which ensures a high

structural efficiency under the specific design loads. However, those space frames have certain shortcomings. When the actual loads are different from the design loads, the nodes of the 3D frameworks may undergo considerable bending moments, and the safety of the structure relies heavily on the nodal bending resistance. Moreover, when it comes to complex irregular space frames, the unique geometries of bars and nodes usually lead to high costs during fabrication and assembly.

It's worth noting that the forms found through PGS have intrinsic planarity that can be harnessed for the

design of sheet-based structure systems, which can avoid the issues brought by the space frames. Sheet-based systems have certain advantages over space frames because of their material accessibility, processibility, low cost, and applicability to large scales [2]. Sheet materials can be easily processed by various fabrication techniques such as laser cutting, CNC milling, CNC bending, waterjet cutting, etc. In terms of structural performance, a sheet-based system provides more stability and is less vulnerable to various loading scenarios because the forces can be transferred and distributed across the faces.

1.1. Background and Related Work

The recent development of 3D graphic statics greatly increased the ease of designing spatial structures. There are two subcategories in the realm of 3D graphic statics using reciprocal diagrams, vector-based [3] and polyhedron-based (PGS) [1], which follow different rules in constructing the form and force 3D dualities. The polyhedron-based approach was initially introduced by Rankine [4] and later developed by Maxwell [5]. Compared to the vector-based method, it guarantees the inherent planarity which can be exploited for sheet-based materialization.

Several research projects investigate the design of sheet-based structures and their materialization approach based on PGS. Akbari et al. introduced a novel method that translates a cellular polyhedral geometry into a polyhedral surface-based manifold structure named shellular structure [12, 13]. The mechanical properties of such structures were studied, and they showed significantly enhanced performance compared to the strut-based cellular structures [14]. A fabrication technique was also proposed based on tucking molecules, a method introduced by Tachi for designing 3D origami [15], and a prototype was made using 0.5mm stainless steel [2]. Akbarzadeh et al. showed the possibility of materializing a 10m- span, modularized glass bridge as a multi-layer system using hollow glass units (HGU) made of 1cm glass sheets [16]. Yost, et al. physically tested the behaviors of one single HGU constructed with 3M™ Very High Bond (VHB) tape as bonding material [17], and the results show that HGU has a significant amount of load capacity. Aiming to address the challenges of large-scale constructions using HGU modules regarding detail developments, fabrication constraints, and assembly logic, Lu et al. presented

the design and fabrication of a 3 m-long double-layer glass bridge prototype [18, 19].

The matrix analysis methods have been created and developed since the 1930s for structural evaluation purposes. For the analysis of frames using the classic forces method, the non-matrix approach initiated by Maxwell [6] has been routinely taught to aerospace, civil, and mechanical engineering students and offers a substantial scope of ingenuity to experienced engineers through a clever selection of redundant force systems [7]. A matrix analysis framework was then found convenient for organizing those calculations. With a focus on pin-jointed spatial frameworks, Pellegrino and Calladine [8] formulated an algorithm that evaluates the performance of the framework rapidly by determining the rank of the kinematic matrix and the bases of its four linear-algebraic vector subspaces. Specifically, it offers complete details of any states of inextensional deformation that a framework may possess. For the face and hinge systems, matrix analysis is also used in the folding simulation of rigid origami, where the loops of bars simulate rigid faces, and the connections between faces act as hinges. The idea of representing triangulated origami as a pin-jointed framework was first proposed by Schenk and Guest [9]. Filipov et al. [10] improved this method with new triangulation schemes for quadrilateral facets. Zhang et al. [11] further generalized the triangulation schemes for any n-gons.

1.2. Problem Statements and Objectives

As shown above, sheet-based structures made through PGS are advantageous because sheet elements constrain the nodal kinematic degrees of freedom and provide more load paths. However, not all sheet elements in the form generated through PGS are necessary as long as the load paths are preserved, and the system does not have kinematic degrees of freedom. By removing redundant sheets, the material cost can be reduced, and the structural efficiency can be further improved.

The design principle is inspired by trusses, where the beam members are connected in a way that they are geometrically restrained. Therefore, when a truss is loaded, the forces are mostly transferred through the axial directions of the beam members without needing much nodal bending resistance. Similarly, for a sheet-based system, this geometric restraining effect is desired such that its load-bearing capacity does not rely much on the edge bending resistance.

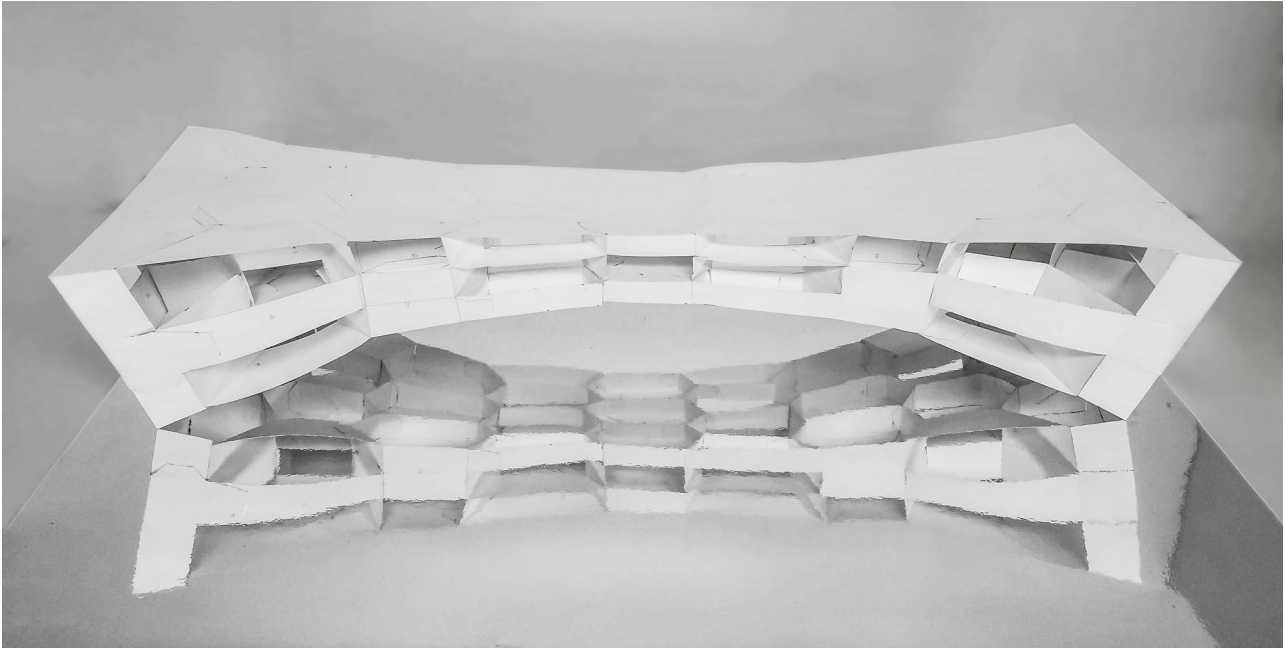


Figure 1: A small-scale physical model made of Bristol paper

In more technical terms, this “restraining” effect can be described as zero kinematic degrees of freedom, meaning that there is no mechanism in the structure. In order to know whether a structure is kinematically determinate or indeterminate, the matrix analysis method is incorporated for kinematic analyses. The matrix analysis method has been used to analyze pin-jointed inextensional frameworks. In this paper, it is adapted for the analysis of rigid face and frictionless hinge systems because a rigid face can be simulated by a cluster of kinematically determinate pin-jointed bars. The performance of this face-hinge system is a good indicator of the performance of a real engineering structure constructed with rigidly connected sheet materials. Zero kinematic degrees of freedom implies a structure with more stability and better performance. This adapted matrix analysis approach is then incorporated into a computational pipeline to help find an efficient set of faces adequate for the construction of a kinematically determinate face-hinge structure (Figure 1).

1.3. Contributions

Based on PGS, this paper introduces a method for designing sheet-based funicular structures that are featured as lightweight and multi-layer. There are several main contributions: first, it provides a new way of utilizing PGS for designing efficient sheet-based structures; second, it adapts the matrix analysis method for the kinematic analysis of face and hinge structural system; finally, a computational pipeline is created as a tool that can be exploited by designers.

2. METHOD

This section is organized into three parts. First, the base geometry is generated using PGS. Next, the matrix analysis method is adapted for the kinematic analysis of sheet-based structures. This is then incorporated into a computational workflow that helps determine an efficient group of faces adequate to keep the kinematic stability and load paths.

2.1. Base Geometry Preparation: Form-Finding through Polyhedral Graphic Statics

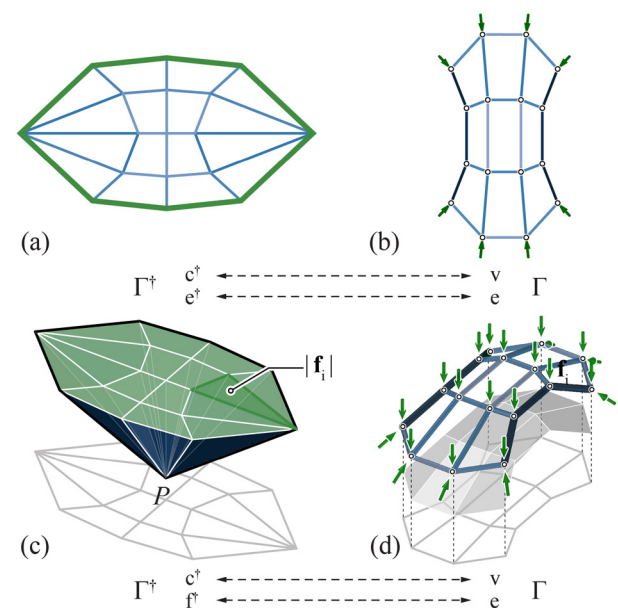


Figure 2: Form-finding of a single-layer funicular shell

The workflow starts with form-finding using PGS. In this section, a single-layer funicular shell is used as an example for the explanation and demonstration of the design principles (Figure 2). As mentioned earlier, the intrinsic planarity allows the form to be delivered as a faceted shell in addition to a space frame (Figure 2d). The goal is to find an efficient set of faces that does not have any mechanisms while maintaining the structural form, i.e., keeping all the load paths. Not all faces in the original faceted geometry are needed to achieve the kinematic determinacy, hence a computational pipeline is devised to help find a reduced number of faces that satisfy the requirements.

2.2. Matrix Analysis Method and Adaptation

Before diving into the details of the computational pipeline, the matrix analysis method for pin-jointed inextensional framework and its adapted method for face-and-hinge structures are explained first as they are the basis of the computational pipeline. The kinematic analysis of a pin-jointed inextensional framework starts from the assembly of the kinematic matrix following the steps formulated by Pellegrino and Calladine [8]. The form can be depicted with 3 characteristics: v vertices connected by e edges and constrained by k kinematic constraints (each defined as one constrained degree of freedom in X, Y, or Z directions) to a rigid foundation.

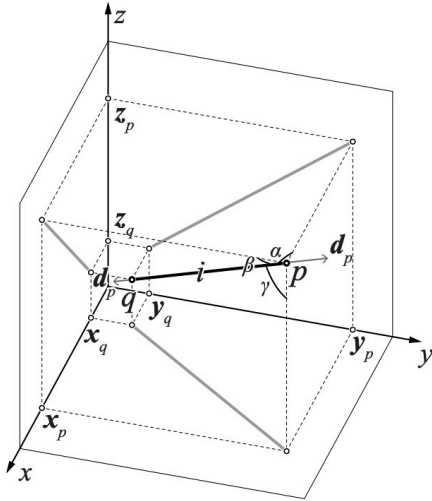


Figure 3: An example edge and the geometric attributes describing nodal displacements and edge elongation

There are also two sets of kinematic variables to be considered: the elongation δ_i for each edge i , and the displacements d_{jx}, d_{jy}, d_{jz} along X, Y, and Z axes in 3D Euclidean space for each vertex j . Their relationship (illustrated in Figure 3) can be written as

$$\delta_i \times l_i = (x_p - x_q)d_{px} + (y_p - y_q)d_{py} + (z_p - z_q)d_{pz} - (x_p - x_q)d_{qx} - (y_p - y_q)d_{qy} - (z_p - z_q)d_{qz} \quad (1)$$

where l_i is the length of edge i , p and q are the endpoints of edge i . Assemble all equations for the e edges in matrix form as

$$\Delta = \mathbf{A} \cdot \mathbf{d} \quad (2)$$

Here Δ is the vector of e elongation coefficients, each defined as $\delta_i \times l_i$

$$\Delta = \begin{pmatrix} \delta_1 \times l_1 \\ \vdots \\ \delta_i \times l_i \\ \vdots \\ \delta_e \times l_e \end{pmatrix} \quad (3)$$

\mathbf{A} is the e by $3v-k$ kinematic matrix, written as

$$\mathbf{A}^T = \begin{pmatrix} \vdots & \vdots & \vdots \\ \cdots & x_p - x_q & \cdots \\ \cdots & y_p - y_q & \cdots \\ \cdots & z_p - z_q & \cdots \\ \vdots & \vdots & \vdots \\ \cdots & x_q - x_p & \cdots \\ \cdots & y_q - y_p & \cdots \\ \cdots & z_q - z_p & \cdots \\ \vdots & \vdots & \vdots \end{pmatrix} \quad (4)$$

\mathbf{d} is the vector of $3v-k$ displacements, written as

$$\mathbf{d} = \begin{pmatrix} \vdots \\ d_{px} \\ d_{py} \\ d_{pz} \\ \vdots \\ d_{qx} \\ d_{qy} \\ d_{qz} \\ \vdots \end{pmatrix} \quad (5)$$

The kinematic indeterminacy m , meaning the number of independent mechanisms, can then be determined by the relationship between the numbers of equations and unknowns, where an important concept of rank r_A comes into play:

$$m = 3v - k - r_A \quad (6)$$

It's important to note that, as stated by Pellegrino, the kinematic indeterminacy here may include the rigid body motion of the framework. In other words, when no vertex is constrained to a foundation, a framework will have a kinematic indeterminacy of greater than or equal to 6, including 3 translational and 3 rotational rigid body degrees of freedom. In the scope of this paper, the rigid body motions are named

external kinematic indeterminacy m_{ex} , and the mechanisms at the vertices are named internal kinematic indeterminacy m_{in} . They satisfy the equation

$$m = m_{ex} + m_{in} \quad (7)$$

When detecting the internal mechanisms of the structure, the external indeterminacy m_{ex} should be excluded. The calculation of m_{ex} is based on the k kinematic constraints to the rigid foundation and is omitted here. All examples in this paper are set up with adequate kinematic constraints to the rigid foundation such that m_{ex} is zero. For the example geometry, there are 24 bars, 12 unconstrained vertices, and 4 other vertices set up as fully constrained (Figure 2d). The rank of the kinematic matrix is calculated to be 12, therefore the internal kinematic indeterminacy is 12 given no rigid body motion is possible, indicating that the framework has 12 internal independent mechanisms.

The locations of the mechanisms can then be obtained by solving for the vertices that have potential displacements. Since the edges in the framework are assumed rigid, there is no elongation in any edge, hence Eq.3 can be replaced by

$$\mathbf{0} = \mathbf{A} \cdot \mathbf{d} \quad (8)$$

The potential displacements of the vertices can be obtained by solving for \mathbf{d} , which is equivalent to solving for the null space of \mathbf{A} . With SciPy [20], the 36 by 12 orthonormal basis of the null space can be computed through singular value decomposition (SVD). The linear combination of the 12 columns represents the possible infinitesimal displacements of the unconstrained vertices. If an unconstrained vertex is unmovable, meaning that it's geometrically restrained by other edges, its displacements will always be zero under any linear combinations. Some random displacement scenarios are exaggerated and visualized in Figure 4, and the locations of the mechanisms can be found. As a side note, each displacement scenario is interrelated to a set of external loads that cannot be balanced, the magnitudes and directions of those loads are not discussed in this paper.

When the structure is built with rigid faces, some additional planar constraints are needed. Those constraints can be implemented using helper edges and vertices for the “stiffening” effect. The edges related to each face need to form a rigid body such that the resulting new pin-jointed framework performs like a face and hinge structure (Figure 5).

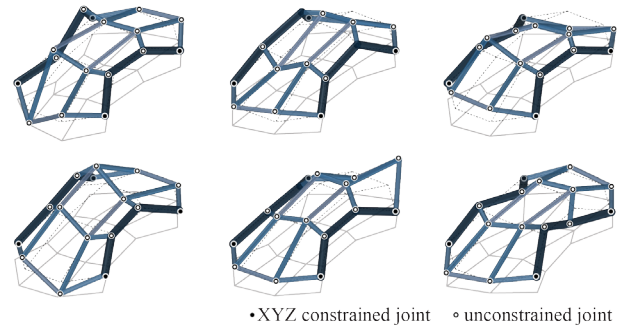


Figure 4: Exaggerated infinitesimal deformations of the framework

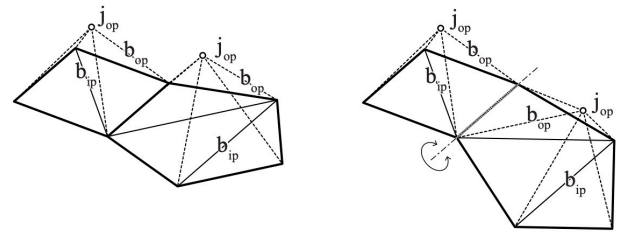


Figure 5: Pin-jointed framework performs like a face-hinge structure

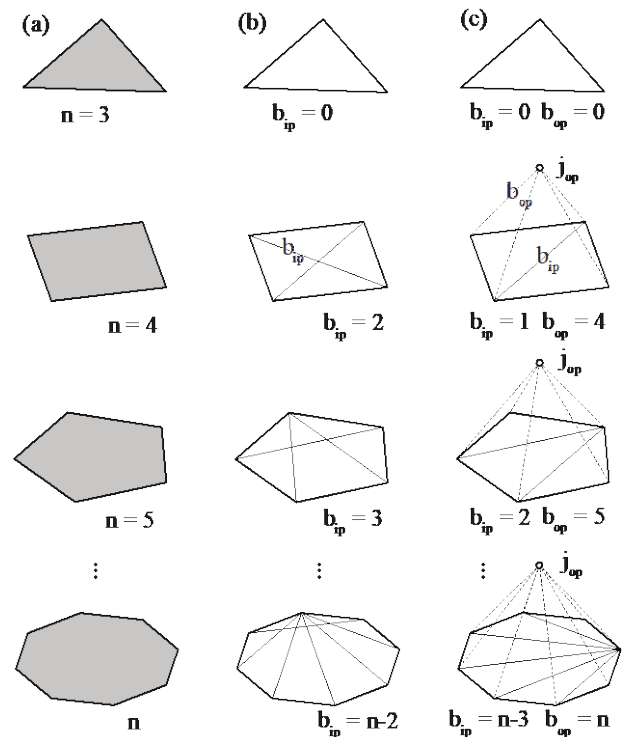


Figure 6: Helper edges and vertices are added for the simulation of rigid faces

The mathematical relationship between the number of required helper edges and the number of polygonal face sides is then established following a method proposed by Zhang et al. [11]. As exploited by [9], a triangular framework can be directly used

for the folding simulation of triangular origami without any helper edges and vertices. For any side count that is larger than 3, helper edges and vertices are needed (Figure 6). Later, the kinematic indeterminacy and locations of mechanisms can be determined for the framework with certain rigid faces. As illustrated in Figure 7, the kinematic indeterminacy of the pin-jointed framework is suppressed with an increasing number of rigid faces, and the framework becomes kinematically stable after 7 rigid faces are added.

2.3. Algorithmic Design

After establishing the analysis method that is compatible with rigid faces, an iterative algorithm is then devised to help determine the reduced group of faces that are sufficient to keep the kinematic stability and load paths. In each iteration, one rigid face is added to the framework, and it stops when the internal kinematic indeterminacy becomes zero. Figure 7 shows the decreased kinematic indeterminacy as more faces are added to the framework. Notably, the sequence of adding rigid faces significantly affects the result of this algorithm. For example, Figure 8a to 8d show 4 cases of adding 7 rigid faces, in which 3 become stable while 1 is still kinematically unstable. Besides, since the goal is to use only sheet materials for the construction of the structure, naked edges are not allowed in the result (Figure 8e). To obtain an efficient number of faces and therefore achieve higher structural efficiency, the sequence of adding rigid faces needs careful consideration. The design of the computational pipeline is illustrated in Figure 9a.

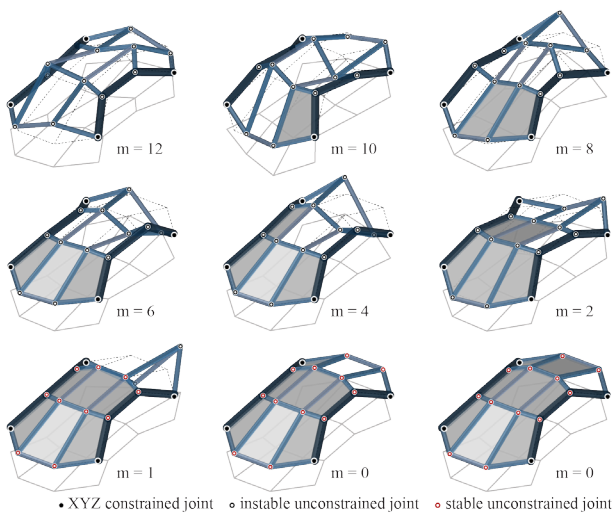


Figure 7: Reduce kinematic indeterminacy with more rigid faces

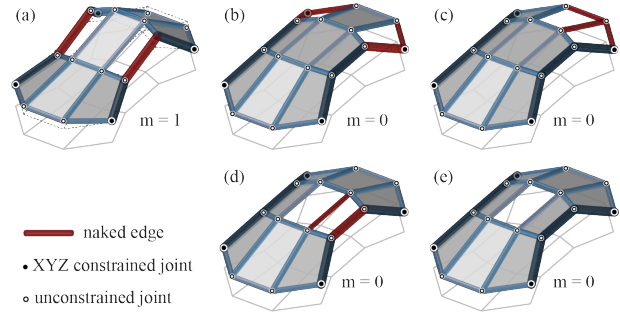


Figure 8: (a)-(d) Kinematic indeterminacies on different sets of 7 faces, (e) the solution without naked edges

The algorithm starts with the input of polyhedral geometry, including all vertices v_i , edges e_i , and faces f_i . The vertices and edges are used to construct the initial framework, and the faces are the candidates to be added. Next, the constraints are set, and the initial m_{in} of the framework is calculated. There is no face stiffened at this point. To help determine the sequence for adding faces, the concept of priority is introduced, where a larger priority means a face will be added first. For each face, its priority pri is calculated based on its area a , the number of neighbor faces f_n , and the number of single-valence edges e_f it has. A larger area leads to a smaller priority because less area means less material and hence higher efficiency. More neighbor faces lead to a larger priority because it tends to reduce more degrees of kinematic indeterminacy. In the case of sheet-only systems, any face with an edge of single-valence, meaning that the edge only belongs to one face candidate, has an infinite priority since it is required to keep the load paths. Based on the description above, the priority function can be formulated as

$$pri = \begin{cases} \infty, & e_f > 0 \\ x(1-a) + yf_n, & e_f = 0 \end{cases} \quad (9)$$

where a is the face area mapped to range 0-1; x and y are coefficients that can be adjusted to tune the weights of a and f_n . Also, this pipeline allows design decisions to be incorporated into the priority function. If certain face candidates are required due to the functionality of the structure, its priority will be overwritten to positive infinite. Contrarily, if any face candidate is unwanted, its priority will be overwritten to zero. After, the priorities of all face candidates are calculated, and the faces are sorted with descending priority. Then, faces are iteratively added to the framework. In each iteration, the face with the highest priority is removed from the list of candidates and “stiffened”. The stiffening is realized

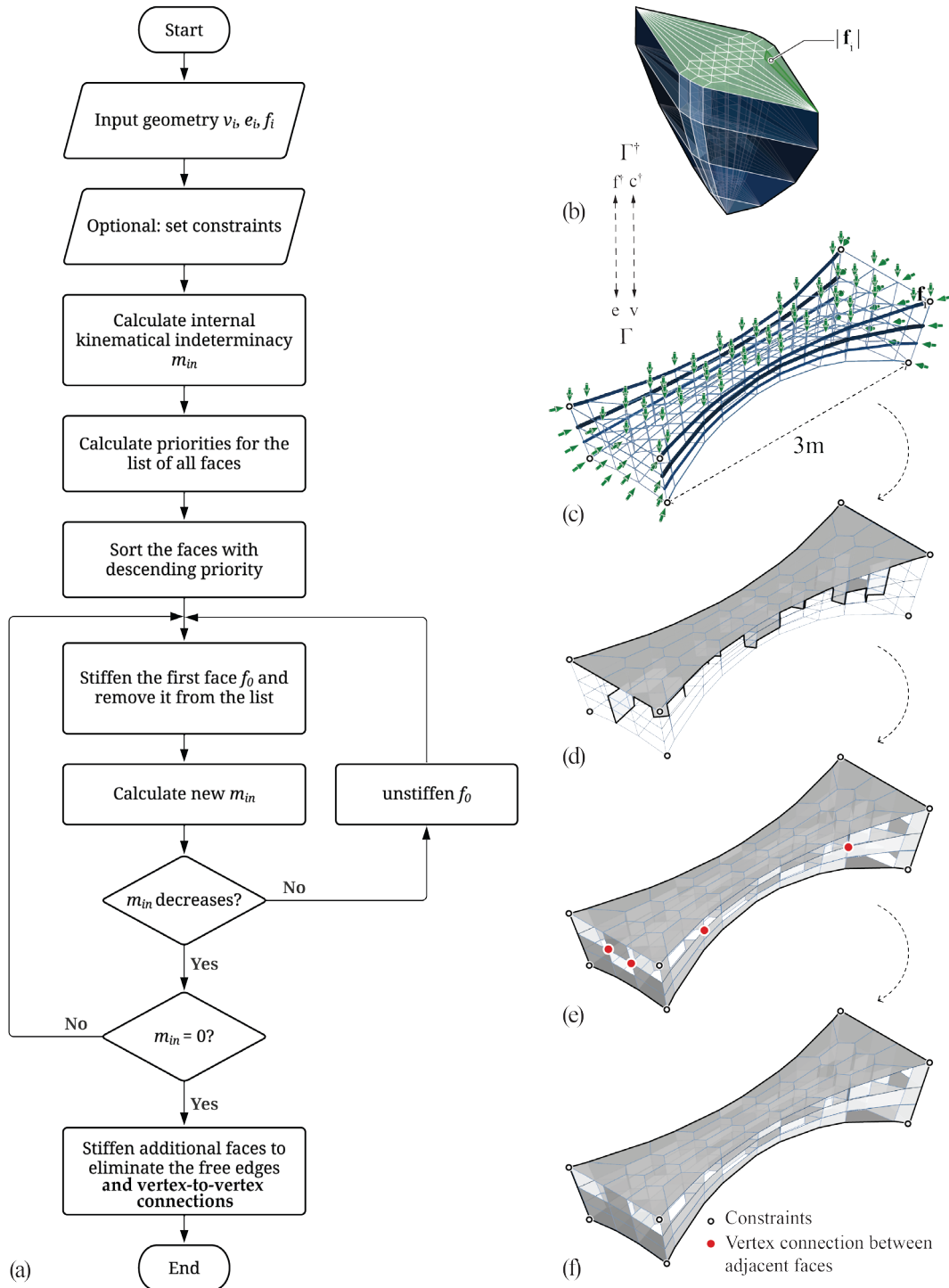


Figure 9: The computational flowchart for determining the faces sufficient to stabilize the framework

by adding helper vertices according to the rule described above in Figure 6. This is then followed by calculating the new m_{in} with all helper vertices and edges. If m_{in} stays the same compared to the last iteration, meaning that this newly added face doesn't help constrain the mechanisms, it will be “unstiffened” by removing the corresponding helper vertex and edges. This process repeats until m_{in}

becomes zero. The final step is to add additional faces in order to eliminate the naked edges and vertex-to-vertex connections (see section 3.1 for more details) since the structure is designed to be built with only sheet materials and the original load. As a result, the output faces function as a kinematically stable face-hinge structure that maintains all primary load paths.

3. CASE STUDY

In this section, the method outlined above is used to design a bridge to attest to the proposed method. A comparative study is carried out using finite element analysis (FEA). A small-scale physical model is also made to explore the connection details between the sheets.

3.1. Base Geometry and Generation Process

The form and force diagrams generated using PGS are shown in Figure 9b, c. 10 kN is used as the total design load applied on the top of the structure, and the total span is set to 3 m. The face-adding process begins after having the base framework geometry. Eight vertices are first chosen as pin anchors to constrain the structure (Figure 9c). No faces are added at this point. Due to its functionality as a bridge, 31 top faces are determined as must-haves for people to walk on. Later, the iterative face-adding algorithm is invoked which finds the additional faces with the least area that reduce the internal kinematic indeterminacy to zero, meaning that there is no mechanism across the structure (Figure 9d). Next, a secondary iterative algorithm is needed to add the minimum set of faces for removing naked edges (Figure 9e). The resulting structure may have vertex-to-vertex connections between adjacent faces as illustrated in Figure 9e, which causes problems for materialization. Therefore, one further action is taken to add additional faces that help eliminate those vertex-to-vertex connections. The final structure is shown in Figure 9f.

3.2. Comparative Numerical Study

To further understand the mechanical performance of the design, a comparative numerical study is carried out on both the sheet-based structure and space frame using the Finite Element Method (FEM). Structural steel is used as the material, and the total material usage is controlled at 66.5 kg for both structures. The structures are simply supported on the vertices of two ends of the bridge, and they are simulated under two static loading scenarios: first under the design load of 10 kN distributed on the top vertices (Figure 10a, b), then under a point load of 3 kN (Figure 10c, d). For the first loading scenario, both structures reported a max displacement below 0.8 mm, and the space frame slightly outperforms the sheet-based structure. For the second loading scenario, the max displacement of the sheet-based structure remains at a low level. However, the space frame reports that of more than 45 mm, indicating a

high risk of failure. The results show that although the sheet-based structure performs slightly worse than the space frame under the design loads, it's potentially more versatile in taking a wider range of loads in real-world applications.

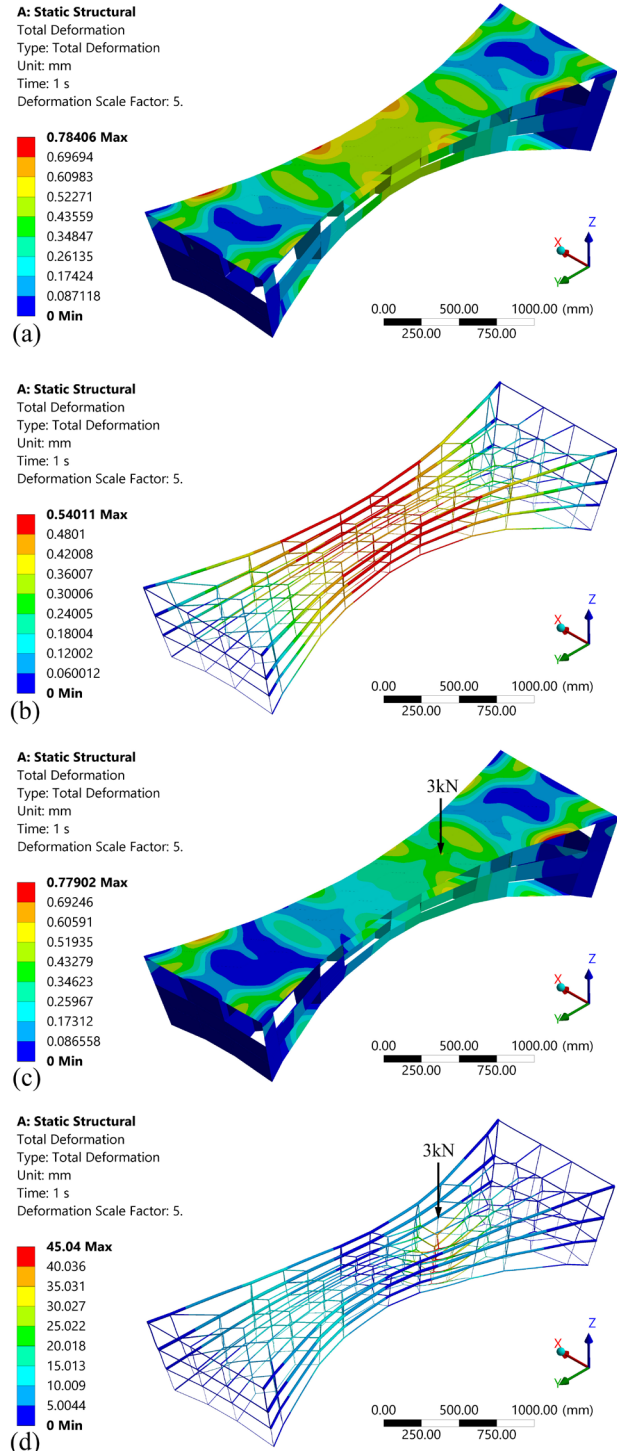


Figure 10: Comparative study with FEA on the sheet-based and framework structures under two load cases

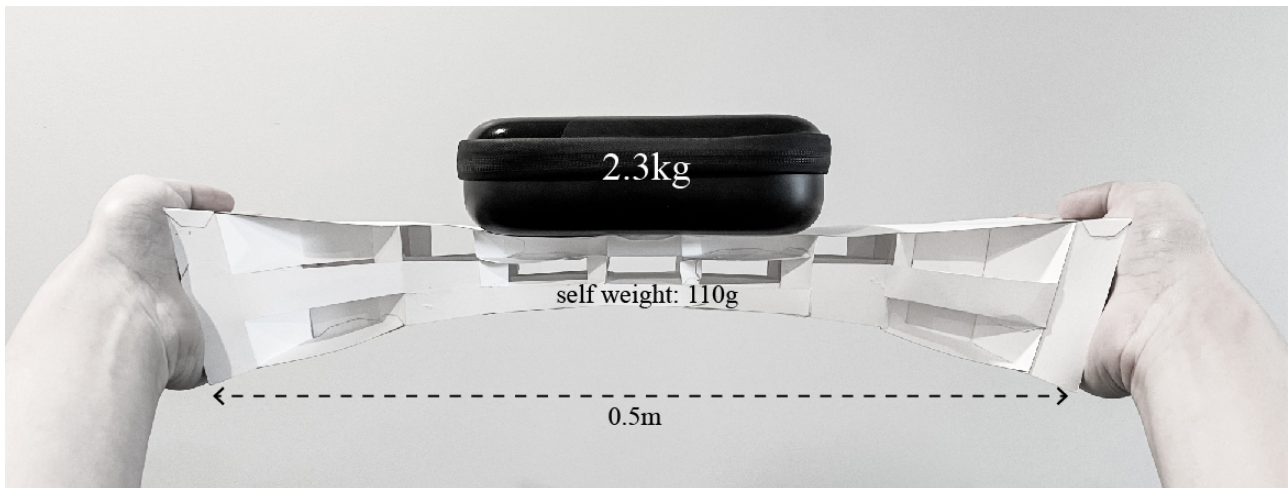


Figure 11: A simple physical load test on the small-scale model made of Bristol paper

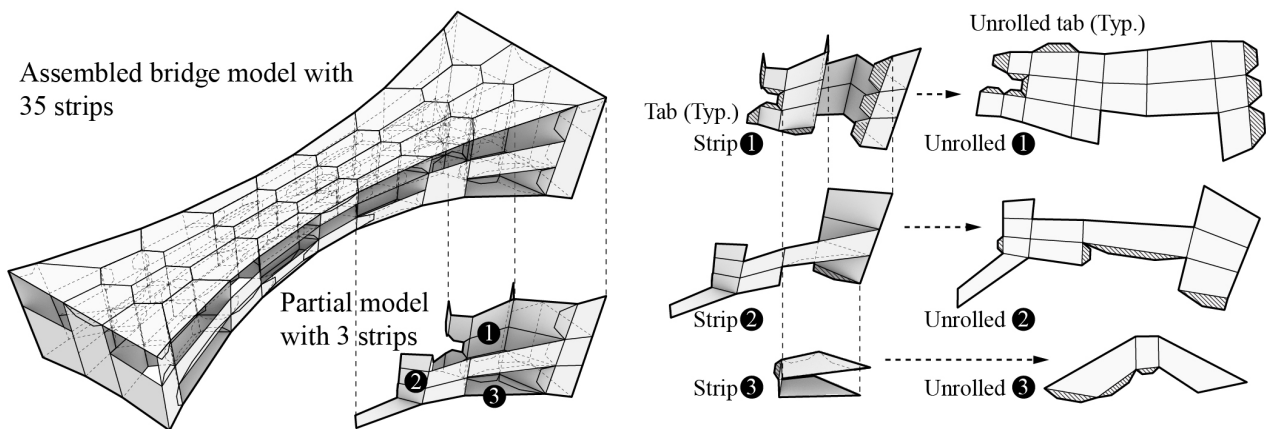


Figure 12: Strips and tabs facilitate the fabrication and assembly of the model

3.3. Small-Scale Physical Model

A 1:6 physical model spanning 0.5 m is made using Bristol paper (Figure 11). For a complex non-manifold geometry like this, two techniques are used to facilitate the fabrication and assembly. First, the total 283 faces are merged into 35 continuous strips and unrolled onto flat sheets such that they can be laser-cut and assembled with fewer parts. Second, all edge connections are realized by small overlaps (tabs) bonded with glue (Figure 12). The model can take 2.3 kg of load with a span of 0.5 m and a self-weight of 110 g, manifesting minor deflections.

4. CONCLUSION AND FUTURE WORK

This paper presents a novel workflow that adapts and combines the matrix analysis method with polyhedral graphic statics to facilitate the design of multi-layer sheet-based lightweight funicular structures with the minimum cost of sheet materials.

The numerical simulation and physical small-scale prototype both show that this system can achieve considerable load capacity with a low material cost. Some materialization strategies are also explored through the physical model. In future steps, the buckling issue of thin sheet materials will be considered in the computational pipeline, and a variety of multi-layer forms will be designed and studied using more comprehensive numerical simulations. Moreover, a larger-scale prototype will be constructed and tested to gain a further understanding of its real-world performance.

ACKNOWLEDGMENTS

The authors gratefully acknowledge the financial support provided by the National Science Foundation CAREER AWARD (NSF CAREER-1944691-CMMI) and the National Science Foundation Future Eco Manufacturing Research Grant (NSF, FMRG-CMMI 2037097) awarded to Dr. Masoud Akbarzadeh.

REFERENCES

- [1] M. Akbarzadeh, 3D Graphical Statics Using Reciprocal Polyhedral Diagrams. PhD thesis, ETH Zurich, 2016. (DOI: 10.3929/ethz-a-010867338)
- [2] M. Akbari, Y. Lu, and M. Akbarzadeh, "From design to the fabrication of shellular funicular structures," in *Proceedings of the Association for Computer-Aided Design in Architecture (ACADIA)*, 2021.
- [3] P. D'Acunto, J.-P. Jasienski, P. O. Ohlbrock, C. Fivet, J. Schwartz, and D. Zastavni, "Vector-based 3D graphic statics: A framework for the design of spatial structures based on the relation between form and forces," *International Journal of Solids and Structures*, vol. 167, pp. 58–70, Aug. 2019. (DOI: 10.1016/j.ijsolstr.2019.02.008)
- [4] W. Rankine, "Principle of the Equilibrium of Polyhedral Frames," *Philosophical Magazine Series 4*, vol. 27, no. 180, p. 92, 1864. (DOI: 10.1080/14786446408643629)
- [5] J. C. Maxwell, "I.—On Reciprocal Figures, Frames, and Diagrams of Forces," *Earth and Environmental Science Transactions of The Royal Society of Edinburgh*, vol. 26, no. 1, pp. 1–40, 1870. Publisher: Royal Society of Edinburgh Scotland Foundation. (DOI: 10.1017/S0080456800026351)
- [6] J. C. Maxwell, "L. On the calculation of the equilibrium and stiffness of frames," *The London, Edinburgh, and Dublin Philosophical Magazine and Journal of Science*, vol. 27, pp. 294–299, Apr. 1864. Publisher: Taylor & Francis. (DOI: 10.1080/14786446408643668)
- [7] C. A. Felippa, "A historical outline of matrix structural analysis: a play in three acts," *Computers & Structures*, vol. 79, pp. 1313–1324, June 2001. (DOI: 10.1016/S0045-7949(01)00025-6)
- [8] S. Pellegrino and C. R. Calladine, "Matrix analysis of statically and kinematically indeterminate frameworks," *International Journal of Solids and Structures*, vol. 22, pp. 409–428, Jan. 1986. (DOI: 10.1016/0020-7683(86)90014-4)
- [9] M. Schenk and S. D. Guest, "Origami Folding: A Structural Engineering Approach," p. 16, 2010.
- [10] E. T. Filipov, K. Liu, T. Tachi, M. Schenk, and G. H. Paulino, "Bar and hinge models for scalable analysis of origami," *International Journal of Solids and Structures*, vol. 124, pp. 26–45, Oct. 2017. (DOI: 10.1016/j.ijsolstr.2017.05.028)
- [11] T. Zhang, K. Kawaguchi, and M. Wu, "A folding analysis method for origami based on the frame with kinematic indeterminacy," *International Journal of Mechanical Sciences*, vol. 146–147, pp. 234–248, Oct. 2018. (DOI: 10.1016/j.ijmecsci.2018.07.036)
- [12] M. Akbari, M. Akbarzadeh, and M. Bolhassani, "From polyhedral to anticlastic funicular spatial structures," in *Proceedings of IAASS Symposium*, 2019.
- [13] M. Akbari, A. Mirabolghasemi, H. Akbarzadeh, and M. Akbarzadeh, "Geometry-based structural form-finding to design architected cellular solids," in *Symposium on Computational Fabrication, SCF '20*, (New York, NY, USA), p. 1–11, Association for Computing Machinery, Nov 2020. (DOI: 10.1145/3424630.3425419)
- [14] M. Akbari, A. Mirabolghasemi, M. Bolhassani, A. Akbarzadeh, and M. Akbarzadeh, "Strut-based cellular to shellular funicular materials," *Advanced Functional Materials*, vol. 32, no. 14, p. 2109725, 2022. (DOI: 10.1002/adfm.202109725)
- [15] T. Tachi, "3d origami design based on tucking molecule," *Origami*, vol. 4, pp. 259–272, 2009.
- [16] M. Akbarzadeh, M. Bolhassani, A. Nejur, J. R. Yost, C. Byrnes, J. Schneider, U. Knaack, and C. B. Costanzi, "The Design of an Ultra-Transparent Funicular Glass Structure," pp. 405–413, Apr. 2019. Publisher: American Society of Civil Engineers. (DOI: 10.1061/9780784482247.037)
- [17] J. R. Yost, M. Bolhassani, P. A. Chhadeh, L. Ryan, J. Schneider, and M. Akbarzadeh, "Mechanical performance of polyhedral hollow glass units under compression," *Engineering Structures*, vol. 254, pp. 113–730, 2022. (DOI: 10.1016/j.engstruct.2021.113730)

- [18] Y. Lu, M. Cregan, P. A. Chhadeh, A. Seyedahmadian, M. Bolhassani, J. Schneider, J. R. Yost, and M. Akbarzadeh, "All glass, compression-dominant polyhedral bridge prototype: form-finding and fabrication," in *Proceedings of IASS Symposium and Spatial Structures Conference 2020/21, Inspiring the next generation*, (Guildford, UK), August 23-27 2021.
- [19] Y. Lu, A. Seyedahmadian, P. A. Chhadeh, M. Cregan, M. Bolhassani, J. Schneider, J. R. Yost, G. Brennan, and M. Akbarzadeh, "Funicular glass bridge prototype: design optimization, fabrication, and assembly challenges," *Glass Structures Engineering*, vol.8, pp.261–272, 2022. (DOI: 10.1007/s40940-022-00177-x)
- [20] P. Virtanen, R. Gommers, T. E. Oliphant, M. Haberland, T. Reddy, D. Cournapeau, E. Burovski, P. Peterson, W. Weckesser, J. Bright, S. J. van der Walt, M. Brett, J. Wilson, K. J. Millman, N. May- orov, A. R. J. Nelson, E. Jones, R. Kern, E. Larson, C. J. Carey, I. Polat, Y. Feng, E. W. Moore, J. VanderPlas, D. Laxalde, J. Perktold, R. Cimrman, I. Henriksen, E. A. Quintero, C. R. Har- ris, A. M. Archibald, A. H. Ribeiro, F. Pedregosa, P. van Mulbregt, and SciPy 1.0 Contributors, "SciPy 1.0: Fundamental Algorithms for Scientific Computing in Python," *Nature Methods*, vol. 17, pp. 261–272, 2020. (DOI: 10.1038/s41592-019-0686-2)